

Studying the single-electron transistor by photoionization

Ioan Bâldea* and Horst Köppel

*Theoretische Chemie, Physikalisch-Chemisches Institut, Universität Heidelberg, Im Neuenheimer Feld 229,
D-69120 Heidelberg, Germany*

(Received 18 November 2008; published 23 April 2009)

We report theoretical results demonstrating that photoionization can be a useful tool for investigating single-electron transistors. It permits to obtain information on the quantum dot occupancy and the charging energy in a direct manner, and not indirectly, as done in transport experiments. It is worth emphasizing that in the photoionization processes considered by us, an electron absorbs a photon with energy of the order of the work functions (~ 1 eV) and is ejected into the vacuum. This phenomenon is completely different from the widely investigated photoassisted tunneling. There, an electron tunnels through a Coulomb island from one electrode to another by absorbing a photon of much lower energy of the order of the charging energy (typically, a few meV). Suggestions are given on how to conduct experiments using photoionization alone or in combination with transport measurements. Monitoring zero kinetic-energy (ZEKE) photoelectrons is especially recommended because ZEKE spectroscopy offers a better resolution than the standard photoemission.

DOI: [10.1103/PhysRevB.79.165317](https://doi.org/10.1103/PhysRevB.79.165317)

PACS number(s): 73.63.Kv, 73.23.Hk, 33.15.Ry, 79.60.Jv

I. INTRODUCTION

In a single-electron transistor (SET), a quantum dot (QD) is coupled via tunneling junctions to metallic electrodes.^{1,2} An isolated QD behaves like an artificial atom, where the electron motion is confined within a small region with size of the order of nanometers.^{3,4} Similar to atoms, the single electron levels of a QD are well-separated energetically. Experiments on SET transport are often interpreted within the Anderson impurity model at equilibrium.⁵⁻⁸ The QD is modeled by a single localized state. Its energy ε_d can easily be tuned by varying the potential V_g of a gate. This approximation is particularly justified in small QDs where single electron levels are well-separated energetically. This state can accommodate $n_d=0, 1$, or 2 electrons. A key quantity for electronic transport through the SET is just this number n_d of (valence) electrons.

Unlike in extended systems, a nonvanishing charging energy $U=e^2/2C$ has to be paid to add one electron to a QD (C is the total capacitance). At sufficiently low temperatures, for a small QD weakly coupled to electrodes, the charging energy U represents the dominant energy scale; it exceeds the thermal energy and the finite width Γ of the dot level resulting from its hybridization (t_d) with electron states of the electrodes.

Therefore, charge fluctuations are largely suppressed and the number of electrons of the dot is an integer in broad ε_d ranges (plateaus): $n_d=0$ for $\varepsilon_d > \varepsilon_F + \Gamma$, $n_d=1$ for $\varepsilon_F - U + \Gamma < \varepsilon_d < \varepsilon_F - \Gamma$, and $n_d=2$ for $\varepsilon_d < \varepsilon_F - U - \Gamma$. The transitions between the states with well-defined dot charge occur within narrow ε_d ranges of width $\sim 2\Gamma$. In these ranges, the QD state is a combination of two nearly degenerate states of well-defined charge (mixed-valence regimes). There, the dot charge can fluctuate and, thus, electron-transport becomes possible. This gives rise to the well-known Coulomb blockade peaks separated by $\Delta\varepsilon_d \approx U$ in the curve of the conductance $G(\varepsilon_d)$ at low temperatures (but larger than the Kondo temperature T_K).⁴ Although charge fluctuations are suppressed within the plateaus, spin fluctuations through virtual

intermediate state are allowed within the (Kondo) plateau where the QD is occupied by one electron ($n_d \approx 1$). At $T < T_K$, they yield a narrow peak (Kondo resonance) in the QD density of states, which enhances the conductance up to the value of the ideal point contact $G_0 = 2e^2/h$ (unitary limit).⁹

The experimental observation of the Coulomb blockade phenomenon and the Kondo effect in electric transport of SETs is remarkable.^{9,10} It indirectly confirms the occurrence of the charge plateaus in broad V_g ranges. This evidence is indirect because what one directly measures in experiment is the conductance G and not the dot charge n_d . Besides, the charging energy U is also indirectly estimated as $\Delta\varepsilon_d \approx U$, while the experimentally measured quantity is V_g and not ε_d .

In the present paper, we shall propose an alternative method to investigate phenomena related to the charge plateaus in a SET, namely, the photoionization. Photoionization is known as a very useful tool to study strong electron correlations.^{11,12} As we shall show, from the investigation of the ionization one can extract more direct information on the QD charge than from transport experiments.

The remaining part of the paper is organized as follows. In Sec. II, we describe the model and present the theoretical results on photoionization. Based on these theoretical results, in Sec. III we suggest possible experiments to employ photoionization as a tool for investigating SETs. Conclusions are presented in Sec. IV.

II. MODEL AND THEORETICAL RESULTS

We shall also describe the SET by the Anderson model,

$$\begin{aligned}
 H = & \varepsilon_F \sum_{\sigma, l=-1}^{-M_L} a_{l, \sigma}^\dagger a_{l, \sigma} + \varepsilon_F \sum_{\sigma, l=1}^{M_R} a_{l, \sigma}^\dagger a_{l, \sigma} \\
 & - t \sum_{\sigma, l=-1}^{-M_L+1} (a_{l, \sigma}^\dagger a_{l-1, \sigma} + \text{H.c.}) - t \sum_{\sigma, l=1}^{M_R-1} (a_{l, \sigma}^\dagger a_{l+1, \sigma} + \text{H.c.}) \\
 & + - t_d \sum_{\sigma} (a_{-1, \sigma}^\dagger d_{\sigma} + a_{+1, \sigma}^\dagger d_{\sigma} + \text{H.c.}) + \varepsilon_d \sum_{\sigma} d_{\sigma}^\dagger d_{\sigma}
 \end{aligned}$$

$$+ U\hat{n}_{d,\uparrow}\hat{n}_{d,\downarrow}, \quad (1)$$

where $a_{l,\sigma}$ ($a_{l,\sigma}^\dagger$) denote annihilation (creation) operators for electrons of spin σ in the left and right leads (L,R), $d_\sigma \equiv a_{0,\sigma}$ ($d_\sigma^\dagger \equiv a_{0,\sigma}^\dagger$) destroys (creates) electrons in the QD, and $\hat{n}_{d,\sigma} \equiv d_\sigma^\dagger d_\sigma$ are electron occupancies per spin direction. The QD-electrode coupling is characterized by the hopping integral t_d , which can be experimentally controlled. In the experimental setup of Ref. 10, t_d can be changed by varying the potential of the gates that form the constrictions, and the dot energy ε_d can be tuned by varying the potential of a “plunger” gate electrode V_g

$$\varepsilon_d = \alpha V_g + \text{const.} \quad (2)$$

The number of electrons will be assumed equal to the number of sites ($N=M_L+M_R+1$). In the photoionization of the QD, a photon of energy ω is absorbed by an electron, which is ejected from the QD into vacuum, and brings the ionized system in one of its eigenstates Ψ_k . The ionization process can be characterized by an energy threshold $\omega_k = \langle \Psi_k | H | \Psi_k \rangle - \langle \Phi | H | \Phi \rangle$ and a spectroscopic factor $f_{k,\sigma}$,

$$f_{k,\sigma} = |\langle \Psi_k | d_\sigma | \Phi \rangle|^2. \quad (3)$$

Here Φ stands for the neutral ground state (case $T=0$). The spectroscopic factor is directly related to the weight of a line in the ionization spectrum, more precisely to the partial-channel ionization cross section.¹¹ From Eq. (3) one can deduce the following sum rule:

$$\sum_k f_{k,\sigma} = \langle \Phi | d_\sigma^\dagger d_\sigma | \Phi \rangle \equiv n_{d,\sigma}. \quad (4)$$

Equation (4) represents an important result. It permits to directly relate the integrated weight of the ionization spectrum to the number of electrons on the QD in the neutral ground-state. From a technical side, Eq. (4) turns out to be very useful to test the numerical results. It allows to check whether the Lanczos algorithm targets all the relevant ionized states Ψ_k .

To compute the ionization spectrum, we shall employ the method of exact numerical (Lanczos) diagonalization. Although this method can only be applied to small electrodes, the results are relevant provided that the number of sites of the electrodes are properly chosen to mimic a metallic behavior.¹³ The single-particle energies of an isolated electrode lie symmetrically around ε_F within the range $(\varepsilon_F - 2t, \varepsilon_F + 2t)$. To ensure that in the ground state of the isolated electrodes the Fermi level is occupied by one electron, one should consider that each electrode consists of an odd number ($M_{L,R}$) of sites. To demonstrate the reduced role of the finite-size effects, we have also considered the QD embedded in a ring ($a_{-M_L,\sigma} \equiv a_{M_R,\sigma}$). In this case, for a similar reason, the ring without the QD should consist of an odd number of sites (odd M_L+M_R). In all numerical results presented here, we set $t=1$. For the numerical calculations, the value of the Fermi energy in electrodes ε_F is not important: it only fixes the energy zero. Therefore, we do not fix the value of ε_F and present in all the figures results for energies relative to ε_F .

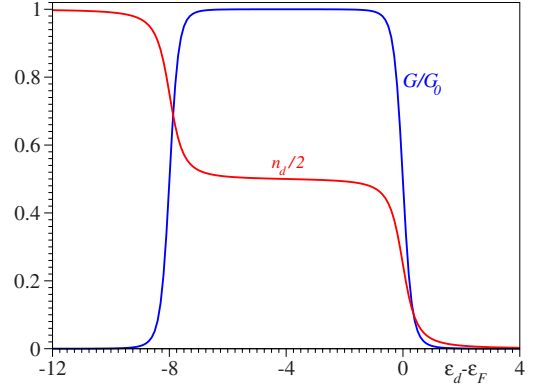


FIG. 1. (Color online) Results for the dot occupancy n_d and normalized conductance G/G_0 for $U=8$, $t_d=0.2$, $t=1$, and $M_L=M_R=5$ ($N=11$). These curves can be hardly distinguished within the drawing accuracy from those for open chains with $(M_L, M_R) = (3, 3)$, $(3, 5)$, and $(3, 7)$, as well as for rings with $N=6, 10$.

Our numerical results for n_d of Fig. 1 demonstrate the formation of broad well-defined charge plateaus ($n_d \approx 0, 1, 2$) separated by narrow mixed-valence regions, as discussed above. The fact that the n_d curve (as well as those for the bright diabatic states, see below) for various electrode sizes and boundary conditions is almost identical within the drawing accuracy in Fig. 1 demonstrates that finite-size effects are not important and the study of small systems is physically relevant. Our extensive numerical results demonstrate that what is essential for the weak finite-size effects is also essential for the occurrence of the charge plateaus, namely, a width parameter $\Gamma \propto t_d^2/t$ smaller than the charging energy U . On this basis, we argue that the charge and the ionization spectra of a QD connected to semi-infinite leads can be accurately deduced by computations for such small “metallic” electrodes.

Although it does not represent a central issue from the present perspective, the weakness of finite-size effects is also relevant for the Kondo effect, which we only mention here in passing. As is well known, essential for the occurrence of this effect is the Kondo screening cloud. The latter extends over a number of sites $\xi_K \sim t/T_K$, which rapidly grows (exponentially for large U) far beyond electrode sizes treatable by the exact numerical diagonalization. Therefore, it is impossible to obtain the conductance within standard transport approaches by employing short electrodes. For semi-infinite electrodes, the zero-bias conductance G can be computed via the Friedel-Langreth sum rule,^{14–16}

$$G = G_0 \sin^2(\pi n_d^\infty / 2) \quad (5)$$

once the dot occupancy n_d^∞ is known. Equation (5) was deduced for a QD attached to semi-infinite leads with a continuum density-of-states, which is the real nanosystem of interest. The pleasant thing is that the zero-bias conductance G for this case can be solely determined from n_d^∞ and a reliable estimated of the latter suffices for this purpose. Fortunately, to this we need not to carry out calculations for semi-infinite or very large electrodes. In view of the weak finite-size effect mentioned above, n_d computed for short electrodes does rep-

resent an accurate estimate $n_d^\infty \approx n_d$. Indeed, the curve for $G(\varepsilon_d)$ obtained by inserting the calculated n_d calculated for short electrodes instead of n_d^∞ —also presented in Fig. 1—has a similar appearance to that obtained by means of the numerical renormalization group^{17,18} for semi-infinite electrodes and nicely reveals the occurrence of the Kondo plateau.

Let us now switch to the results for SET photoionization. To avoid misunderstandings, we emphasize that the photoionization considered in this paper is qualitatively different from the widely studied photoassisted tunneling (see, for example, Ref. 19 and references therein). The process where a photon helps an electron to tunnel from one electrode to another through a Coulomb island might also be viewed as an “ionization” phenomenon. Nevertheless, the scale of the corresponding “ionization” energies is determined by the charging energy U . For semiconducting QDs, it is of the order of ~ 1 meV, that is, much smaller than ionization energies of the order of the work-functions (~ 1 eV) considered by us.

Typical exact numerical results for the ionization energies and spectroscopic factors of all the significant ionization processes are depicted in Fig. 2. To understand these results, it is helpful to analyze first the limit $t_d \rightarrow 0$.

In this limit, two ionization processes of the QD are possible. For $\varepsilon_d < \varepsilon_F - U$, the dot is doubly occupied ($n_d = 2$), and the relevant ionization process consists of removing an electron from the upper Hubbard “band.” The corresponding ionization energy is $\omega_u^0 = -\varepsilon_d - U$. For $\varepsilon_F - U < \varepsilon_d < \varepsilon_F$, the dot is occupied by a single electron in the lower Hubbard band ($n_d = 1$). To remove it, an ionization energy $\omega_l^0 = -\varepsilon_d$ is needed. The corresponding spectroscopic factors are $f_u^0 = 1$ and $f_l^0 = 1/2$.

Basically, the exact results presented in Figs. 2(a) and 2(b) differ from those of this limiting case in two ways. First, in the mixed-valence regimes $\varepsilon_d \approx \varepsilon_F$ and $\varepsilon_d \approx \varepsilon_F - U$, the finite coupling causes a smearing effect similar to that already observed on the curve $n_d(\varepsilon_d)$ in Fig. 1. Second, the exact curves exhibit numerous avoided crossings. In the present case, avoided crossings occur around the points where elementary ionization processes become quasis resonant. All nearly linear pieces of the curves in Fig. 2(a) are reminiscent of elementary ionization processes in the noninteracting case ($t_d \rightarrow 0$). For instance, one-hole processes in electrodes are represented by horizontal lines. Two-hole-one-particle (2h-1p) processes where the creation of one hole in the upper or lower Hubbard band is accompanied by the excitation of a particle-hole pair in electrodes are represented by lines parallel to the ω_u^0 or ω_l^0 lines, respectively. To mention only one more example, 2h-1p processes involving the creation of two holes in the upper and lower Hubbard bands and of one electron in electrodes at or above the Fermi level are represented by the straight line $\omega_l^0 = -2\varepsilon_d - U + \varepsilon_F$ or parallels to it. At the intersection points of such lines, avoided crossings arise rather than true intersections; the latter occurring only for $t_d \rightarrow 0$. As discussed recently,²⁰ avoided crossings are very frequent in tunable QD systems.

Numerous avoided crossings are visible in Fig. 2(a), but for practical purposes they are less important, and therefore

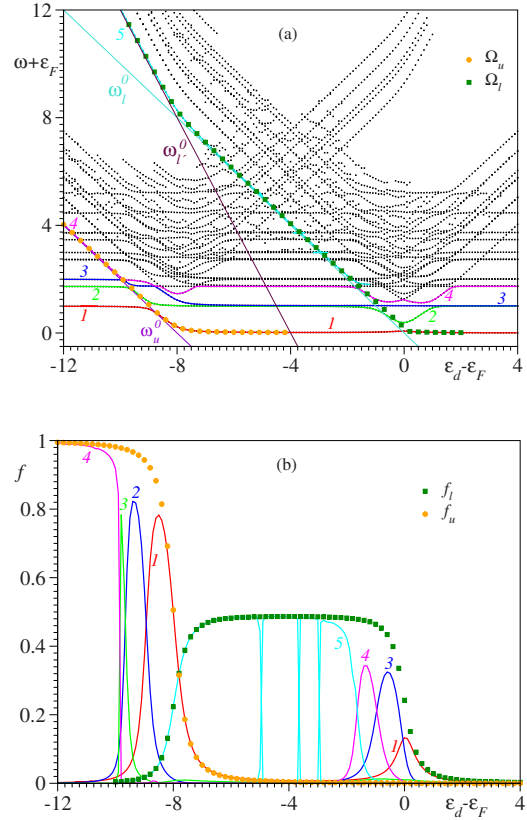


FIG. 2. (Color online) Results for (a) ionization energies and (b) spectroscopic factors. The solid lines 1, 2, 3, and 4 are for the eigenstates with substantial spectroscopic factors. The results for the two relevant diabatic bright states (u, l) are depicted by symbols. The black points in (a), which correspond to the ionized eigenstates with small spectroscopic factors ($10^{-5} \leq f \leq 10^{-2}$), are not quantitatively significant for the ionization spectrum but are showed to better visualize the occurrence of the avoided crossings. Notice that the ionization energies are measured relative to the electrode work function ($-\varepsilon_F$), a quantity much larger than the charging energy U . Parameter values as in Fig. 1. See the main text for details.

only a few are shown in Fig. 2(b). Parts thereof are not important because the spectroscopic factors are too small. But even if the signals are sufficiently intense, avoided crossings are less important. In the narrow regions around the critical points where the intensities are significant, the energy differences are usually smaller than the experimental resolution and only the summed intensities of the participating states can be measured. What one measures is a smoothly varying spectroscopic factor attributed to a bright diabatic state.²⁰ The constant spacings between different families of parallel lines in Fig. 2(a) can be understood by noting that the single-particle energies of the isolated electrodes considered there are ε_F , $\varepsilon_F \pm t$, and $\varepsilon_F \pm t\sqrt{3}$. For long electrodes, bundles of dense parallel lines within a width $4t$ will appear, so of practical interest are just such bright diabatic states passing through a multitude of avoided crossings.

Therefore, besides the results for individual eigenstates, we also show in Figs. 2(a) and 2(b) the curves $\Omega_{u,l}$ and $f_{u,l}$ for the two bright diabatic states that are significant. Deep inside the plateaus, the ionization signals corresponding to

these two diabatic states behave similarly to the case $t_d \rightarrow 0$; but substantial deviations are visible in the mixed-valence regimes. Noteworthy is not only that the spectroscopic factors penetrate the neighboring charge plateaus, where they gradually decrease, similar to n_d (Fig. 1). Even more interesting is the fact that all these penetrations are accompanied by substantial changes in the slope of the $\Omega_{u,l}$ curves.

III. PROPOSED EXPERIMENTS

In view of the present theoretical results, we propose to conduct the following experiments using an intense incoming flux of monochromatic photons, which is well-focused on the QD of a SET. To avoid confusions, we emphasize again that the photons should have energies of the order of the work-functions, significantly higher than of the microwave and rf fields considered in the previous studies on SETs and the Anderson model.

(i) The first type of experiments is a standard ionization study. To measure the absorption coefficient would be desirable but presumably a too hard task. Probably it would be easier to measure the zero kinetic-energy (ZEKE) photoelectrons emitted from the dot at the ionization threshold, as in threshold ionization experiments in molecular physics. Just because the QD is very small, not only photoelectrons from the QD but also from electrodes will be inherently ejected into vacuum. Therefore, it is important but, fortunately, easy to experimentally distinguish between the ionization of the QD and that of the electrodes. By varying the gate potential V_g , the ionization energies ω_i change in the former case [$\omega_i \approx -\varepsilon_d(V_g)$ and $\omega_i \approx -\varepsilon_d(V_g) - U$] but remain constant in the latter ($\omega_i = -\varepsilon_F$). Let us analyze the change in ionization by gradually increasing the dot energy ε_d starting from a sufficiently low value, by making V_g more and more negative. In the first stage, an ionization signal will be observed, which is characterized by a nearly constant intensity I_u ($I_u \propto \tilde{f}_u \approx 1$). Its intensity will drop to zero within a narrow range $\delta V_{g1} \sim 2\Delta V$ ($\Delta V = -\Gamma/\alpha > 0$) centered on $V_g = V_{g1}$. A little before this signal disappears, another ionization signal will appear at $V_g \sim V_{g1} + \Delta V$, whose intensity rapidly rises to a value $I_l \approx I_u/2$ ($I_l \propto \tilde{f}_l \approx 0.5$) beyond $V_g \sim V_{g1} - \Delta V$. Further on, this intensity remains nearly constant up to a point where it rapidly falls down to zero within a range $\delta V_{g2} \sim 2\Delta V$ centered on $V_g = V_{g2}$. Except for the mixed-valence ranges δV_{g1} and δV_{g2} , the corresponding ionization energies $\Omega_u(V_g)$ and $\Omega_l(V_g)$ are straight lines of the same slope. This slope is half the slope of the $\Omega_l(V_g)$ curve in the range $V_{g1} < V_g < V_{g1} + \Delta V$. At the other end, $V_{g2} - \Delta V < V_g < V_{g2}$, this curve tends to saturate $\Omega_l(V_g) \rightarrow -\varepsilon_F$. The same tendency of the other curve [$\Omega_u(V_g) \rightarrow -\varepsilon_F$] can be seen in the opposite mixed-valence range $V_{g1} - \Delta V < V_g < V_{g1}$. By extrapolating the linear parallel portions of the $\Omega_{u,l}$ curves ($\Omega_{u,l} \rightarrow \tilde{\Omega}_{u,l}$), one can directly determine the charging energy from the difference of their ordinates taken at the same value of V_g , $U = \tilde{\Omega}_u(V_g) - \tilde{\Omega}_l(V_g)$.²¹ Noteworthy, for this, the values of V_g or ε_d themselves are not needed. This represents an important difference from the determination of U in transport experiments. In the latter, what one can directly measure the values V_{g1}

and V_{g2} from the positions where the Coulomb blockade peaks occur at temperatures $T \geq T_K$ or from the extension of the Kondo plateau observable for $T < T_K$. The determination of U from the difference $V_{g1} - V_{g2}$ alone is impossible and to this aim the relationship between V_g and ε_d [Eq. (2)] is necessary. There is still another important difference between ionization and transport measurements. As visible in Fig. 2(a), $\Omega_u(V_{g1}) \approx \Omega_l(V_{g2}) \approx -\varepsilon_F$. The Fermi energy can thus be estimated. This is also important because this quantity can alternatively be deduced from the ionization energy $-\varepsilon_F$ of the electrodes (electrode work-function). To conclude, the V_g -dependent ionization spectrum allows one to give direct evidence on the formation of the charge plateaus and to determine the quantities U , Γ , and ε_F . The dependence $\varepsilon_d(V_g)$ can also be obtained, which is also important, as it allows to quantitatively investigate the capacitances of nanosystems.

(ii) A (ZEKE) ionization study might be difficult, but a mixed ionization-transport experiment as proposed below is presumably easier while still relevant. In a usual transport experiment, one can measure the conductance as a function of the gate potential $G(V_g)$ and determine V_{g1} and V_{g2} , say, from the Kondo plateau ($T < T_K$). At a fixed gate potential $V_{g2} < V_g < V_{g1}$, one can now shine the QD with radiation whose frequency ω is varied. At a certain value of the latter, $\omega = \omega_c(V_g)$, the incoming photon will ionize the QD. Because the single (unpaired) electron of the QD will be ejected, the Kondo effect will be suppressed, and this will be evidenced by the drop in the conductance ($G \approx 0$). From the above considerations, one expects a linear V_g dependence of $\omega_c(V_g) \equiv \Omega_l(V_g)$. Again, the charging energy can be directly determined as $U = \tilde{\Omega}_l(V_{g1}) - \tilde{\Omega}_l(V_{g2})$. The dependence of ε_d on V_g is not needed rather it can be deduced by this method, as well as the Fermi energy $\varepsilon_F = -\tilde{\Omega}_l(V_{g2})$.

(iii) A similar mixed experiment can be imagined at $V_g < V_{g2}$, where the nonionized QD is doubly occupied. At the resonant photon frequency $\omega = \Omega_u(V_g)$, one electron will be removed. For a sufficiently intense irradiation, one can reach a stationary state where the ionized QD will be occupied by an unpaired electron. Because the latter is a prerequisite for the occurrence of the Kondo effect, it is tempting to speculate on a possible photoionization-induced nonequilibrium Kondo effect; thence, an effect of photoionization opposite to that of suppressing the equilibrium Kondo effect discussed above.

IV. CONCLUSION

In this paper, we have showed that photoionization is a valuable method, which can be used along with transport measurements, to study SETs. To our knowledge, conductance measurements represent the only way to determine the charging energy U , which thus resembles very much a fit parameter. Therefore, the comparison with the result of a completely different method is quite meaningful, even more if U is obtained in a direct manner and not via a supplementary relation between ε_d and V_g . For specific purposes, photoionization turns out to provide even richer information than transport studies.

The above considerations refer to a QD with a single level. However, from the physical analysis it is clear that the results are also relevant for more general situations.

Another important result is that QD ionization can be accurately described by considering short electrodes (weak finite-size effects), and only very few ionized states are

relevant. Both aspects are very important, since they urge to carry out realistic *ab initio* calculations on photoionization, particularly for single-molecule-based SETs.

The authors acknowledge with thanks the financial support for this work provided by the Deutsche Forschungsgemeinschaft (DFG).

*Also at National Institute for Lasers, Plasmas, and Radiation Physics, Institute for Space Sciences, RO 077125 Bucharest, Romania; ioan@pci.uni-heidelberg.de

¹T. A. Fulton and G. J. Dolan, Phys. Rev. Lett. **59**, 109 (1987).

²D. Goldhaber-Gordon, H. Shtrikman, D. Mahalu, D. Abusch-Magder, U. Meirav, and M. A. Kastner, Nature (London) **391**, 156 (1998).

³M. A. Kastner, Phys. Today **46**(1), 24 (1993).

⁴L. Kouwenhoven and C. Marcus, Phys. World **11**, 35 (1998).

⁵D. V. Averin and K. K. Likharev, J. Low Temp. Phys. **62**, 345 (1986).

⁶T. K. Ng and P. A. Lee, Phys. Rev. Lett. **61**, 1768 (1988).

⁷L. I. Glazman and M. E. Raikh, JETP Lett. **47**, 452 (1988).

⁸W. Izumida, O. Sakai, and Y. Shimizu, J. Phys. Soc. Jpn. **67**, 2444 (1998).

⁹W. G. van der Wiel, S. de Franceschi, T. Fujisawa, J. M. Elzerman, S. Tarucha, and L. P. Kouwenhoven, Science **289**, 2105 (2000).

¹⁰D. Goldhaber-Gordon, J. Gores, M. A. Kastner, H. Shtrikman, D.

Mahalu, and U. Meirav, Phys. Rev. Lett. **81**, 5225 (1998).

¹¹L. S. Cederbaum, W. Domcke, J. Schirmer, and W. Von Niessen, Adv. Chem. Phys. **65**, 115 (1986).

¹²I. Bâldea and L. S. Cederbaum, Phys. Rev. Lett. **89**, 133003 (2002).

¹³I. Bâldea and H. Köppel, Phys. Rev. B **78**, 115315 (2008).

¹⁴D. C. Langreth, Phys. Rev. **150**, 516 (1966).

¹⁵H. Shiba, Prog. Theor. Phys. **54**, 967 (1975).

¹⁶Y. Meir and N. S. Wingreen, Phys. Rev. Lett. **68**, 2512 (1992).

¹⁷W. Izumida, O. Sakai, and S. Suzuki, J. Phys. Soc. Jpn. **70**, 1045 (2001).

¹⁸T. A. Costi, Phys. Rev. B **64**, 241310(R) (2001).

¹⁹T. Mii, K. Makoshi, and H. Ueba, Surf. Sci. **493**, 575 (2001).

²⁰I. Bâldea and L. S. Cederbaum, Phys. Rev. B **77**, 165339 (2008).

²¹Because typically $U \sim 1$ meV and $\tilde{\Omega}_{u,l} \sim 1$ eV, it is advantageous to use ZEKE spectroscopy, which has a better resolution than the standard photoemission.